

Collapse of Landau level in semi-Dirac materials

Daniil Asafov¹ and Ilia Pavlov²

¹*California Institute of Technology, Pasadena, California 91125, USA*

²*School of Physics and Engineering, ITMO University, 197101 St. Petersburg, Russia*

(Dated: February 21, 2024)

Two-dimensional semi-Dirac models describe a family of novel materials that have anisotropic dispersion with relativistic-type spectrum along one of the spatial directions and non-relativistic along another. In the present paper we perform a detailed analysis of Landau levels collapse for such models in perpendicular magnetic field and in-plane electric field by using semi-classical approach and tight-binding simulations. The anisotropic nature of semi-Dirac dispersion manifests itself in the possibility of Landau level collapse for only one of the electric field directions. In addition, the topological transition with merging Dirac cones has its own distinct features in Landau level collapse.

I. INTRODUCTION

The topological transition in novel two-dimensional materials with two Dirac cones moving and merging at one point in momentum space attracted great attention in the literature [1–3]. The corresponding systems are called semi-Dirac systems and support quasiparticles with effective Hamiltonian having relativistic-type linear dispersion along one direction in momentum space and non-relativistic quadratic dispersion along another direction. Several effective semi-Dirac models were used to describe physics in the black phosphorus [4–9]. In the simplest versions of semi-Dirac models the additional gap parameter controls whether two bands will be separated, touching in one point or two Dirac cones will appear [6, 7, 10–12]. There is a number of experimental realizations of such systems in optical lattices [13] and in microwave cavities [14]. Typically the parameters of setup can be tuned to demonstrate different types of quasiparticle spectrum in the same system. Many physical properties of semi-Dirac materials were studied in recent years: among them the optical conductivity for different types of semi-Dirac systems [6–9, 15, 16], the magnetoconductivity [17, 18], thermoelectric response [19] Hall conductivity [20] and the unusual scaling of Landau levels with magnetic field [2, 3].

In the present paper we concentrate our attention on phenomena of collapse of Landau levels in an in-plane electric field for the semi-Dirac system. Firstly the presence of such phenomenon was discovered for relativistic quasiparticles in graphene [21, 22]. It was found that When the electric field strength approaches certain critical value, the formal solutions for Landau levels becomes singular. The gap-separated Landau levels are expected to disappear, and the continuous spectrum is instead formed. Such effect can be also understood in terms of Lorentz transformation, when the effective moving frame speed coincides with the speed of massless quasiparticles [21, 23, 24]. Later the Landau level collapse was observed experimentally by measuring the field when Shubnikov-de-Haas oscillations disappear for the given sample [25]. Later it was found, that also radial

electric field can lead to similar collapse effect [24].

There is a number of differences in collapse of Landau levels that are expected for semi-Dirac system comparing to more typical Dirac semimetals. The main difference is caused by anisotropic structure of the spectrum, which itself should lead to anisotropy in critical values of electric field. In addition, a set of two quasiclassically disconnected parts of Fermi surface is present in the cases of two separated Dirac cones [2, 3, 7], and one may expect an additional effect of tunneling that will modify Landau level collapse in such a case. The open question of how Landau level collapse happens in semi-Dirac models motivate the study in the present paper.

The paper is organized as follows: in Sec. II we recall the main properties of low-energy semi-Dirac model with gap parameter that controls topological phase transition. Next, in Sec. III we present a semi-classical calculations of Landau levels that appear in crossed electric and magnetic field. Additionally, we present asymptotic analysis for exact Schrödinger equation for such system. The special attention is given to the case when the tunneling (also called magnetic breakdown) takes part and modifies the structure of quasiclassical Landau levels. The corresponding calculations are presented in Sec. IV. Finally, in Sec. V we compare the results with those known for graphene and give concluding remarks.

II. SEMI-DIRAC MODEL AND TOPOLOGICAL TRANSITION WITH MERGING DIRAC CONES

The effective Hamiltonian that captures separated Dirac cones and gapped regime as well as topological transition between them is given by the following expression:

$$H = (\Delta + ak_x^2)\sigma_x + vk_y\sigma_y. \quad (1)$$

There are a number of modifications of this Hamiltonian with higher-order terms or additional gap parameters with another matrix structure [9]. Here we analyze the simplest version of such Hamiltonian, which was called ‘universal’ in Refs. [2, 3] as it captures the essential

physics of Landau level collapse. The dispersion for each of two bands in the absence of external fields is given by

$$\varepsilon_{\pm}(\mathbf{k}) = \pm \sqrt{(ak_x^2 + \Delta)^2 + v^2 k_y^2}. \quad (2)$$

The two band-touching Dirac points are separated by the distance $\delta_x = 2\sqrt{\Delta/a}$ in momentum space along x-direction in the case of negative $\Delta < 0$ assuming $a, v > 0$. In the case of zero gap parameter $\Delta = 0$ the two bands touch at $\mathbf{k} = 0$.

III. SEMI-CLASSICAL QUANTIZATION OF CYCLOTRON ORBITS AND MAGNETIC BREAKDOWN

The description of Landau levels in the effective model given by Hamiltonian (1) was presented in Ref.[3]. The main features such as scaling with magnetic field and Landau level index can be captured by using Peierls-Onsager quasiclassical quantization rule, which states that the area of the constant energy curve in momentum space should be quantized

$$S(\varepsilon(\mathbf{k}) = \text{const}) = 2\pi(N + \gamma)eB. \quad (3)$$

As was pointed out in [26], the presence of electric field modifies the Peierls-Onsager quantization rule:

$$S(\varepsilon(\mathbf{k}) - \mathbf{v}_d \mathbf{k} = \text{const}) = 2\pi(N + \gamma)eB, \quad (4)$$

with classical drift velocity in crossed fields defined as $\mathbf{v}_d = c\mathbf{E} \times \mathbf{B}/B^2$. Before proceeding with more detailed calculations let us perform qualitative analysis. The collapse of Landau levels is associated with the fact that the area defined by contour in momentum space $\varepsilon - \mathbf{v}_d \mathbf{k} = \text{const}$ becomes infinite. This may happen either for Landau level with particular index or for all levels simultaneously. Consequently, the general criteria for the presence of Landau level collapse for the band spectrum in infinite momentum space $-\infty < k_{x,y} < \infty$ is equivalent to the question of existence of closed curve of solutions for equation $\varepsilon(\mathbf{k}) - \mathbf{v}_d \mathbf{k} = \text{const}$ with fixed right-hand side constant. The geometrical interpretation of this criteria can be formulated in terms of shape of cross-section of the dispersion $\varepsilon(\mathbf{k})$ by the plane $\mathbf{v}_d \mathbf{k} + \text{const} = 0$, as illustrated on the figure [1]. Such cross-section becomes an open curve when the dispersion grows slower than linear with pre-factor \mathbf{v}_d at large momenta values:

$$\varepsilon(\mathbf{k} \rightarrow \infty) \lesssim \mathbf{v}_d \mathbf{k}. \quad (5)$$

This formula allows one to predict the existence of Landau level collapse by analyzing the asymptotic behavior of dispersion.

Applying (5) to the dispersion of semi-Dirac model and taking asymptotics along two orthogonal directions,

$$\varepsilon_+(k_x \rightarrow \infty) \sim ak_x^2, \quad \varepsilon_{\pm}(k_y \rightarrow \infty) \sim \pm vk_y, \quad (6)$$

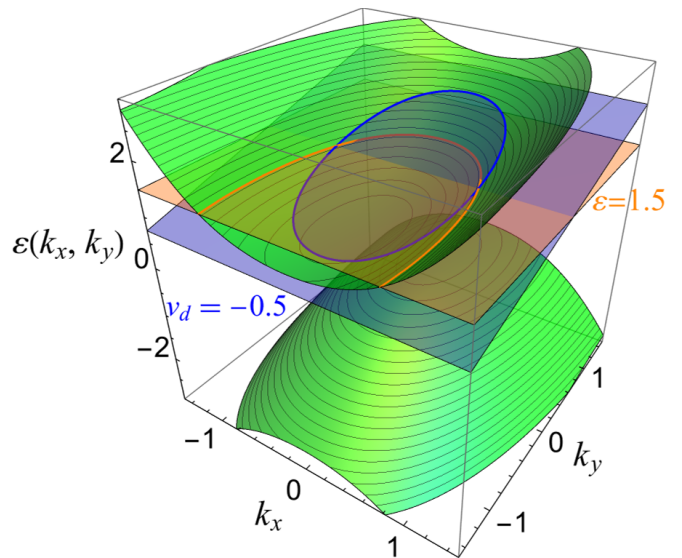


FIG. 1: Spectrum given by the equation 2. The gap parameter is $\Delta = 1$. We choose units $v = 1, a = 1$. Two planes on the picture represent additional $\mathbf{v}_d \mathbf{k}$ part from the 4. As illustrated by the blue plane, when v_d is the small intersection of the plane and the spectrum figure is a closed orbit and thus, Landau-level exists. However, when v_d is very large, as with the orange plane, the intersection is an open orbit and therefore we can say that we observed the collapse of Landau levels.

we find that collapse of Landau level is possible for the case of drift velocity having a nonzero component along the y-direction. The collapse happens for all energy levels simultaneously when this component is bigger than the parameter of the model $v_{d,y} > v$. For the case of the uniform constant electric and magnetic field with B-field along the z-direction, this leads to the fact that the electric field should have a nonzero component along x direction, with critical value for the collapse:

$$E_{x,c} = vB_z/c. \quad (7)$$

For the electric field directed along y-axis of the model, the collapse of Landau levels is not possible.

IV. ENERGY LEVELS IN THE PRESENCE OF ELECTROMAGNETIC FIELD

To calculate energy levels we will use the equation 4. Full technical calculations are given in the appendix A, but the main idea is to notice, that the resulting closed orbit could be described by the equation

$$\left(\frac{k_x^2}{2m} + \Delta\right)^2 + (v_F^2 - v_d^2) \left(k_y - \frac{v_d \mathcal{E}^*(\mathbf{p})}{v_F^2 - v_d^2}\right)^2 = \frac{v_F^2}{v_F^2 - v_d^2} \mathcal{E}^{*2} \quad (8)$$

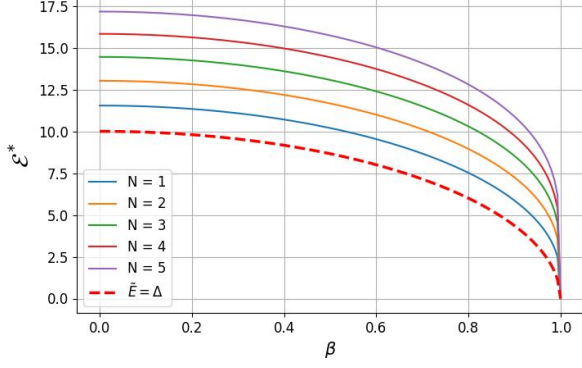


FIG. 2: Numerical solution for the equation 10 with $\Delta = mv_F^2 = \frac{eB}{mc}$. Here $\beta = \frac{v_d}{v_F}$ and \mathcal{E}^* is measured in the units of $\frac{eB}{mc}$

Denoting $\tilde{E} = \frac{v_F}{\sqrt{v_f^2 - v_d^2}} \mathcal{E}^*$ and $(k_y - \frac{v_d \mathcal{E}^*(\mathbf{p})}{v_F^2 - v_d^2})$ we can express the area of the orbit as

$$S(k_x, k_y) = \int \int dk_x d\tilde{k}_y \theta \left(\tilde{E}^2 - \left(\frac{k_x^2}{2m} + \Delta \right)^2 - (v_F^2 - v_d^2) \tilde{k}_y^2 \right) \quad (9)$$

In the case of $\Delta \geq 0$ the equation for energy levels has the form

$$\frac{\pi(|\tilde{E}| - \Delta) \sqrt{|\tilde{E}| + \Delta}}{4\sqrt{a}\sqrt{v^2 - v_d^2}} F\left(\frac{1}{2}, \frac{3}{2}, 3, -\frac{|\tilde{E}| - \Delta}{|\tilde{E}| + \Delta}\right) = 2\pi(N + \gamma) \frac{eB}{c} \quad (10)$$

. This equation can be solved numerically. On the figure 2 we plot the solution for a particular Δ , but the whole form is quite general for the case $\Delta \geq 0$.

In the case of negative gap parameter $\Delta < 0$ the effective dispersion (2) contains two Dirac points separated in momentum space. As a result, there are two closed "orbits" possible (see figure 3)

In this situation there is a possibility of tunneling between two orbits which influences the energy levels structure. The tunneling probability decays exponentially with the energy deviation from the saddle point level. Thus, we should implement double-well representation to properly describe the semi-classical spectrum around that point. The complete theory of corresponding semi-classical description was presented in Ref.[27]. Here we use the quantization condition derived from this description:

$$\cos \left[\frac{\Omega_1 + \Omega_2}{2} + \phi(\mu) \right] = |\mathcal{T}(\mu)| \cos \left[\frac{\Omega_1 - \Omega_2}{2} \right]. \quad (11)$$

$\Omega_j = \pi + \frac{eB}{c} S_j + \int_0^1 \frac{\tilde{H}_1^{\nu(t_j)}}{v_x^{\nu(t_j)}} dk dt_j + (-1)^{j+1} \delta_y^B$. S_j - is the area of the corresponding orbit, $\tilde{H}_1 = H_1^R + H_1^Z + H_1^B - H_1(0)$ - correspond to Roth, Zeeman and Berry

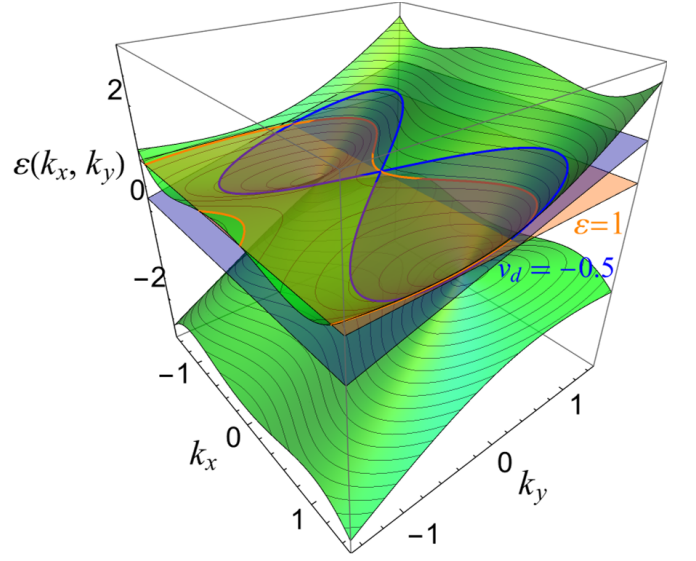


FIG. 3: Spectrum given by the equation 2 with the parameter $\Delta = -1$. We notice that by regulating the electrical field strength two independent closed figures can emerge.

corrections and δ_y^B is an additional Berry phase. Since in our case Berry curvature is equal to zero and the Zeeman Hamiltonian is absent the only term left is the area of the orbit in k -space S_j . Noticing that the areas of the orbits are identical, we get the expression:

$$\cos \left[\frac{c}{eB} S + \phi(\mu) \right] = -\frac{e^{\pi\mu/2}}{\sqrt{2} \cosh \pi\mu}. \quad (12)$$

The area of an orbit can be calculated by the same method we used earlier. Denoting $\delta = \frac{|\tilde{E}|}{\Delta}$ and using the equation A4 we obtain

$$S = \frac{\sqrt{2m} |\Delta|^{\frac{3}{2}} \delta^2 \sqrt{1 - \delta}}{2\sqrt{v_F^2 - v_d^2}} F\left(\frac{1}{2}, \frac{3}{2}, 3, -\frac{2\delta}{1 - \delta}\right) \quad (13)$$

Using the definition of ϕ and μ from the [27]

$$\phi(\mu) = \arg[\Gamma(\frac{1}{2} - i\mu)] + \mu(\ln(|\mu|) - 1) \quad (14)$$

$$\mu = \pm \sqrt{\frac{2m}{v_F^2 - v_d^2} \frac{c|\Delta|^{\frac{3}{2}}}{eB} (1 - \delta)} \quad (15)$$

Where \mp corresponds to the branch choice in the equation 2. Solving this final equation numerically, we get the structure of energy levels described on the figure ???. One can notice, that the conditions for Landau-levels collapse does not depend on Δ and happens when $\beta = 1$.

One can observe a peculiar effect: the birth of pairs of energy levels with the increase of the electrical field. The mathematical origin of such a solution can be illustrated

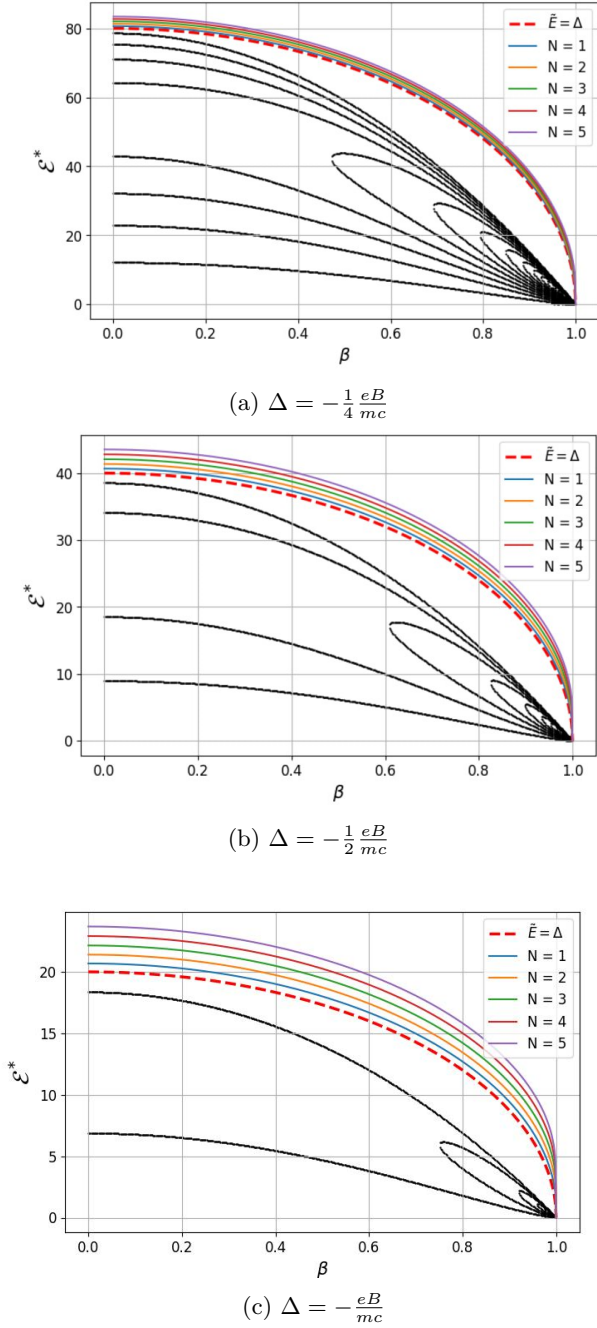


FIG. 4: Numerical solution for the equation 12 + in the equation 2. High energy levels have the same structure as on the figure 2, however, below the level $\bar{E} = |\Delta|$ we get a different structure, including the emergence of "loops". As before, $\beta = \frac{v_d}{v_F}$, $\Delta = -2mv_F^2$ and \mathcal{E}^* is measured in the units of $\frac{eB}{mc}$. The magnetic field being increased two times from picture to picture. The stronger magnetic field is the less levels below the saddle point we have

pretty straightforwardly.

Let us take the limit $\mu \gg 1$ in the equation 12, which arises at relatively small energies and large fields. In this limit, we can use the form of Stirling's approximation for complex arguments with large absolute value (see chapter IV in [28]) and expand $\arg[\Gamma(\frac{1}{2} - i\mu)] \approx -\mu(\ln \mu - 1)$. Then, the equation 12 turns into

$$\cos \left[\frac{c\sqrt{2m}|\Delta|^{\frac{3}{2}}}{2eB\sqrt{v_F^2 - v_d^2}} \delta^2 \sqrt{1 - \delta} F\left(\frac{1}{2}, \frac{3}{2}, 3, -\frac{2\delta}{1 - \delta}\right) \right] = -1 \quad (16)$$

Denoting $\frac{c\sqrt{2m}|\Delta|^{\frac{3}{2}}}{2eB\sqrt{v_F^2 - v_d^2}}$ as $\tilde{\omega}$ we can rewrite the equation as

$$\cos \left[\tilde{\omega} \delta^2 \sqrt{1 - \delta} F\left(\frac{1}{2}, \frac{3}{2}, 3, -\frac{2\delta}{1 - \delta}\right) \right] = -1 \quad (17)$$

Now, let's denote the function $f(\delta) = \delta^2 \sqrt{1 - \delta} F\left(\frac{1}{2}, \frac{3}{2}, 3, -\frac{2\delta}{1 - \delta}\right)$ and look at this function at the point $\delta = \delta_0$, such that $\frac{d}{d\delta} f(\delta) = 0 \Big|_{\delta=\delta_0}$. Figure 5 suggests that there is only one point like that. This point is also an extremum for the function $\cos[\tilde{\omega} f(\delta)]$. Moreover, this is an extremum of that function for any $\tilde{\omega}$. We can see that because the function $f(\delta)$ is continuously growing on the interval $(0, \delta_0)$ and is continuously decaying on the $(\delta_0, 1)$ different $\tilde{\omega}$ just correspond to different oscillation frequencies and thus two different number of times the cosinus function touches the line $f(\delta) = -1$. The new pair of levels is born whenever $\cos(\tilde{\omega} f(\delta_0)) = -1$. From here we can write the condition on birth of a pair of levels as

$$\sqrt{1 - \beta_*^2} = \frac{c\sqrt{2m}|\Delta|^{\frac{3}{2}}}{2eBv_F} \frac{f(\delta_0)}{\pi + 2\pi n} \quad (18)$$

Where β_* are the values of $\frac{v_d}{v_f}$ at which new pairs of levels are born. Numerical calculations of $f(\delta_0) = 0.155829$. The observed appearance of pairs of energy levels with

growing electric field can be understood in the following way: this phenomenon happens on the level of saddle point, where the tunneling effects are strong. For a typical Landau level the orbit remains closed with changing electric field, thus Landau level energy moves to the lower energy. In the case of Landau levels near saddle point the orbit might pass the saddle point level and break down. Such modified quantization rule might allow for the appearance of new allowed Landau levels when the effective dispersion \mathcal{E}^* deforms under the growing electric field.

V. CONCLUSIONS

To summarise, we have analyzed the semi-Dirac model subjected to in-plane electric and out-of-plane magnetic field and found the condition for the appearance of Landau level collapse phenomenon. Based on a semiclassical

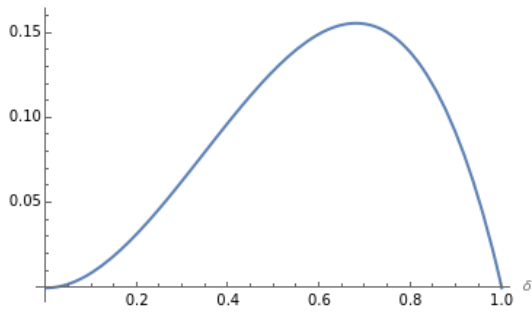


FIG. 5: Plot of the function $f(\delta)$

WKB-type approach, we found that the Landau level collapse appears only when the effective dispersion grows as linear function of momentum or slower. Application of this general criteria as well as exact derivation of semi-classical Landau level dispersion from the constant energy curves modified by electric field have shown that the LL collapse happens only for one direction of elec-

tric field. In other words, only electric field with the x-component exceeding the threshold leads to LL collapse. This result can be contrasted with the example of monolayer graphene, where any direction of electric field has possibility to make a collapse.

In addition, we analyzed the structure of LL for electric field values close to collapse for the gap parameter of the model corresponding to three topologically distinct cases (two Dirac cones, one band touching point and two gapped bands). We have discovered that in the case of the negative gap parameter $\Delta < 0$ the number of Landau levels below the saddle point increases.

VI. ACKNOWLEDGMENTS

We would like to express our gratitude to Leonid Levitov and Dmytro Oriekhov for the idea of the project and for their guidance and help. We would also like to thank Yelizaveta Kulynych for helpful discussions.

Appendix A: Evaluation of area integrals for semi-classical quantization

The effective dispersion of semi-Dirac model has the form

$$\mathcal{E}(\mathbf{p}) = \pm \sqrt{\left(\frac{k_x^2}{2m} + \Delta\right)^2 + v_F^2 k_y^2}. \quad (\text{A1})$$

It predicts the relativistic dispersion along one direction and non-relativistic along another (and mix in between). The "unusual" power law comes from the anisotropy of the model and the corresponding constant energy curve area function with energy. The Landau level collapse happens when electrical field has the component $E_x > \frac{v_f}{c} H$. The E_y component has no effects on the collapse.

Let us find semiclassical energy levels in the presence of electrical field. The modified dispersion [26]

$$\mathcal{E}^*(\mathbf{p}) = \pm \sqrt{\left(\frac{k_x^2}{2m} + \Delta\right)^2 + v_F^2 k_y^2} - v_d k_y = \text{const} \quad (\text{A2})$$

In order to find areas in the momentum space it is convenient to rewrite this equation as

$$\left(\frac{k_x^2}{2m} + \Delta\right)^2 + (v_F^2 - v_d^2) \left(k_y - \frac{v_d \mathcal{E}^*(\mathbf{p})}{v_F^2 - v_d^2}\right)^2 = \frac{v_F^2}{v_F^2 - v_d^2} \mathcal{E}^{*2} \quad (\text{A3})$$

From this equation it is clear the electrical field corresponds only to scaling of energy levels, and does not lead to other significant effects. It is worth noting that here we can see the collapse arising at $v_d = v_F$.

Let us denote in the following calculations that $\frac{v_F^2}{v_F^2 - v_d^2} \mathcal{E}^{*2} = \tilde{E}^2$ and $\left(k_y - \frac{v_d \mathcal{E}^*(\mathbf{p})}{v_F^2 - v_d^2}\right) = \tilde{k}_y$. The area of orbit in the momentum space can be calculated as

$$S(k_x, k_y) = \int \int dk_x d\tilde{k}_y \theta(\tilde{E}^2 - \left(\frac{k_x^2}{2m} + \Delta\right)^2 - (v_F^2 - v_d^2) \tilde{k}_y^2) \quad (\text{A4})$$

There are two cases we need to study: $\Delta \geq 0$ and $\Delta < 0$. Let us start with the first case. The integral comes down to

$$S(k_x, k_y) = \frac{2}{\sqrt{v_F^2 - v_d^2}} \int_{-\sqrt{2m}\sqrt{|\tilde{E}| - \Delta}}^{\sqrt{2m}\sqrt{|\tilde{E}| - \Delta}} \sqrt{\tilde{E}^2 - \left(\frac{k_x^2}{2m} + \Delta\right)^2} dk_x \quad (\text{A5})$$

And can be transformed to

$$S(k_x, k_y) = \frac{2\sqrt{2m}(|\tilde{E}| - \Delta)^{\frac{3}{2}}}{\sqrt{v_F^2 - v_d^2}} \int_{-1}^1 \sqrt{\frac{\tilde{E}^2}{(|\tilde{E}| - \Delta)^2} - (x^2 + \frac{|\tilde{E}|}{(|\tilde{E}| - \Delta)} - 1)^2} dx \quad (\text{A6})$$

From here, changing the integration variable to $d(x^2)$ and using the integral representation of the hypergeometric function

$$F(a, b, c, z) = \frac{\Gamma(c)}{\Gamma(b)\Gamma(c-b)} \int_0^1 t^{b-1} (1-t)^{c-b-1} (1-zt)^{-a} dt \quad (\text{A7})$$

We get, that

$$S(k_x, k_y) = \frac{2\sqrt{2m}(|\tilde{E}| - \Delta)\sqrt{|\tilde{E}| + \Delta}}{\sqrt{v_F^2 - v_d^2}} F\left(\frac{1}{2}, \frac{3}{2}, 3, -\frac{|\tilde{E}| - \Delta}{|\tilde{E}| + \Delta}\right) = 2\pi \frac{eB}{c} (n + \gamma) \quad (\text{A8})$$

When the $\Delta < 0$ an interband breakdown for some energy levels can arise, so our quantization rule should be modified.

When $|\frac{\tilde{E}}{\Delta}| = \delta \geq 1$ formula A8 holds for negative Δ as well. However, when $\delta < 1$ there exist two closed classical orbits and there is a possibility of tunnelling between them. This case is described in the paper [27]

$$\cos \left[\frac{\Omega_1 + \Omega_2}{2} + \phi(\mu) \right] = |\mathcal{T}(\mu)| \cos \left[\frac{\Omega_1 - \Omega_2}{2} \right]. \quad (\text{A9})$$

In our case, with the absence of Berry's curvative and Zeeman hamiltonian Ω_1 and Ω_2 are just equal to the dimensionless surfaces of both trajectories in the momentum space. As we can see from the equation A4 the Surfaces are equal to each other. Using the equation A4 we obtain four possible "stop points" - the integration limits for surface calculation: $k_x = \pm \sqrt{2m(|\Delta| \pm |\tilde{E}|)}$. Transforming to dimensionless variables we get

$$S_1 = S_2 = \frac{2\sqrt{2m}|\Delta|^{\frac{3}{2}}}{\sqrt{v_F^2 - v_d^2}} \int_{-\sqrt{1-\delta}}^{-\sqrt{1+\delta}} \sqrt{\delta^2 - (x^2 - 1)^2} dx \quad (\text{A10})$$

Changing the integration variable to $\frac{x^2-1}{\delta}$ and expanding the expression as $(\delta + 1 - x^2)(\delta + x^2 - 1)$ we will get

$$S = \frac{2\sqrt{2m}|\Delta|^{\frac{3}{2}}\delta^2}{\sqrt{v_F^2 - v_d^2}} \int_{-1}^1 \sqrt{(1-x)(1+x)(1+\delta x)} dx \quad (\text{A11})$$

From here it is easy to obtain the integral representation of a hypergeometric function A7 by changing the integration variable to $\frac{1+x}{2}$ and as a result we get

$$S = \frac{\sqrt{2m}|\Delta|^{\frac{3}{2}}\delta^2\sqrt{1-\delta}}{2\sqrt{v_F^2 - v_d^2}} F\left(\frac{1}{2}, \frac{3}{2}, 3, -\frac{2\delta}{1-\delta}\right) \quad (\text{A12})$$

μ , $\phi(\mu)$ and $\mathcal{T}(\mu)$ we take as defined in the paper [27]

$$\mu = \pm \sqrt{\frac{2m}{v_F^2 - v_d^2} \frac{c|\Delta|^{\frac{3}{2}}}{eB}} (1 - \delta) \quad (\text{A13})$$

Where choice of the sign corresponds to the brunch choice in the equation A2 (Note, that equation A12 includes both brunches due to the modulus of \tilde{E}).

$$\phi(\mu) = \text{arg}[\Gamma(\frac{1}{2} - i\mu)] + \mu(\ln(|\mu|) - 1) \quad (\text{A14})$$

$$\mathcal{T}(\mu) = e^{i\phi(\mu)} \frac{e^{\pi\mu/2}}{\sqrt{2} \cosh \pi\mu} \quad (\text{A15})$$

And the only thing we left to do is to put them into this final equation

$$\cos\left[\frac{c}{eB}S + \phi(\mu)\right] = -\frac{e^{\pi\mu/2}}{\sqrt{2}\cosh\pi\mu} \quad (\text{A16})$$

An approximate solution of this equation could be found with the right estimation for $\arg[\Gamma(\frac{1}{2} - i\mu)]$. To find this estimation, we use the Weierstrass's definition of the Gamma function

$$\Gamma(z) = \frac{e^{-\gamma z}}{z} \prod_{n=1}^{\infty} \left(1 + \frac{z}{n}\right)^{-1} e^{z/n} \quad (\text{A17})$$

Where γ is the Euler–Mascheroni constant

Let's define the phase ϕ_n as $(z+n) = |z+n|e^{i\phi_n}$. Then, according to [A17](#)

$$\arg[\Gamma(\frac{1}{2} - i\mu)] = \gamma\mu - \phi_0 - \sum_{n=1}^{\infty} \left(\frac{\mu}{n} + \phi_n\right) \quad (\text{A18})$$

Where we can take $\phi_n = -\arcsin\left(\frac{\mu}{\sqrt{(n+\frac{1}{2})^2 + \mu^2}}\right)$. Using the approximation $\sum_{n=1}^{\infty} f(n) \approx \int_1^{\infty} f(x)dx$ for slowly changing functions (which applies to $\frac{1}{x}$ when $x \geq 1$) we get

$$\arg[\Gamma(\frac{1}{2} - i\mu)] \approx \gamma\mu + \arcsin\frac{\mu}{\sqrt{\frac{1}{4} + \mu^2}} + \int_1^{\infty} \left(\arcsin\frac{\mu}{\sqrt{(x+\frac{1}{2})^2 + \mu^2}} - \frac{\mu}{x}\right) dx \quad (\text{A19})$$

Expanding $\arcsin\left(\frac{\mu}{\sqrt{(x+\frac{1}{2})^2 + \mu^2}}\right) = x' \arcsin\left(\frac{\mu}{\sqrt{(x+\frac{1}{2})^2 + \mu^2}}\right)$ we get

$$\int \arcsin\left(\frac{\mu}{\sqrt{(x+\frac{1}{2})^2 + \mu^2}}\right) dx = x \cdot \arcsin\left(\frac{\mu}{\sqrt{(x+\frac{1}{2})^2 + \mu^2}}\right) + \frac{\mu}{2} \ln(\mu^2 + (x+\frac{1}{2})^2) + C$$

And, therefore

$$\arg[\Gamma(\frac{1}{2} - i\mu)] \approx \gamma\mu + \mu - \frac{\mu}{2} \ln(\mu^2 + \frac{9}{4}) + \arcsin\frac{\mu}{\sqrt{\frac{1}{4} + \mu^2}} - \arcsin\frac{\mu}{\sqrt{\frac{9}{4} + \mu^2}} \quad (\text{A20})$$

Now, let us look at two asymptotics $|\mu| \gg 1$ and $|\mu| \ll 1$. Expanding [A20](#) for both cases we get

$$\begin{aligned} \phi(\mu) &\approx \gamma\mu, \text{ when } |\mu| \gg 1 \\ \phi(\mu) &\approx (\gamma + \ln\frac{3}{2})\mu + \mu \ln|\mu|, \text{ when } |\mu| \ll 1 \end{aligned} \quad (\text{A21})$$

The equation [A16](#) turns into

$$\begin{aligned} \cos\left(\frac{c}{eB}S + \gamma\mu\right) &\approx 1, \text{ when } |\mu| \gg 1 \\ \cos\left(\frac{c}{eB}S + (\gamma + \ln\frac{3}{2})\mu + \mu \ln|\mu|\right) &\approx \frac{1}{\sqrt{2}} - \frac{\pi}{2}\mu, \text{ when } |\mu| \ll 1 \end{aligned} \quad (\text{A22})$$

-
- [1] Y. Hasegawa, R. Konno, H. Nakano, and M. Kohmoto, Zero modes of tight-binding electrons on the honeycomb lattice, [Physical Review B](#) **74**, 033413 (2006).
[2] G. Montambaux, F. Piéchon, J.-N. Fuchs, and M. O. Goerbig, Merging of Dirac points in a two-dimensional crystal, [Physical Review B](#) **80**, 153412 (2009).
[3] G. Montambaux, F. Piéchon, J.-N. Fuchs, and M. O. Goerbig, A universal Hamiltonian for motion and merging of Dirac points in a two-dimensional crystal, [The European Physical Journal B](#) **72**, 509 (2009).
[4] M. Ezawa, Highly anisotropic physics in phosphorene, [Journal of Physics: Conference Series](#) **603**, 012006 (2015).

- [5] P. K. Pyatkovskiy and T. Chakraborty, Dynamical polarization and plasmons in a two-dimensional system with merging Dirac points, *Physical Review B* **93**, 085145 (2016).
- [6] J. P. Carbotte, K. R. Bryenton, and E. J. Nicol, Optical properties of a semi-Dirac material, *Physical Review B* **99**, 115406 (2019).
- [7] J. P. Carbotte and E. J. Nicol, Signatures of merging Dirac points in optics and transport, *Physical Review B* **100**, 035441 (2019).
- [8] P. Adroguer, D. Carpentier, G. Montambaux, and E. Orignac, Diffusion of Dirac fermions across a topological merging transition in two dimensions, *Physical Review B* **93**, 125113 (2016).
- [9] J. Jang, S. Ahn, and H. Min, Optical conductivity of black phosphorus with a tunable electronic structure, *2D Materials* **6**, 025029 (2019).
- [10] E. Illes, J. P. Carbotte, and E. J. Nicol, Hall quantization and optical conductivity evolution with variable Berry phase in the $\alpha - T_3$ model, *Physical Review B* **92**, 245410 (2015).
- [11] E. Illes and E. J. Nicol, Magnetic properties of the $\alpha-t_3$ model: Magneto-optical conductivity and the Hofstadter butterfly, *Physical Review B* **94**, 10.1103/physrevb.94.125435 (2016).
- [12] D. O. Oriekhov and V. P. Gusynin, Optical conductivity of semi-dirac and pseudospin-1 models: Zitterbewegung approach, *Phys. Rev. B* **106**, 115143 (2022).
- [13] L. Tarruell, D. Greif, T. Uehlinger, G. Jotzu, and T. Esslinger, Creating, moving and merging Dirac points with a Fermi gas in a tunable honeycomb lattice, *Nature* **483**, 302 (2012).
- [14] M. Bellec, U. Kuhl, G. Montambaux, and F. Mortessagne, Topological transition of Dirac points in a microwave experiment, *Physical Review Letters* **110**, 033902 (2013).
- [15] K. Ziegler and A. Sinner, Lattice symmetries, spectral topology and opto-electronic properties of graphene-like materials, *EPL (Europhysics Letters)* **119**, 27001 (2017).
- [16] A. Mawrie and B. Muralidharan, Direction-dependent giant optical conductivity in two-dimensional semi-Dirac materials, *Physical Review B* **99**, 075415 (2019).
- [17] X. Zhou, W. Chen, and X. Zhu, Anisotropic magneto-optical absorption and linear dichroism in two-dimensional semi-Dirac electron systems, *Physical Review B* **104**, 235403 (2021).
- [18] P. Sinha, S. Murakami, and S. Basu, Landau levels and magneto-optical transport properties of a semi-dirac system, *Phys. Rev. B* **105**, 085401 (2022).
- [19] I. Mandal and K. Saha, Thermoelectric response in nodal-point semimetals, arxiv 10.48550/arXiv.2309.10763 (2023).
- [20] P. Sinha, S. Murakami, and S. Basu, Quantum hall studies of a semi-dirac nanoribbon, *Phys. Rev. B* **102**, 085416 (2020).
- [21] V. Lukose, R. Shankar, and G. Baskaran, Novel electric field effects on landau levels in graphene, *Phys. Rev. Lett.* **98**, 116802 (2007).
- [22] N. M. R. Peres and E. V. Castro, Algebraic solution of a graphene layer in transverse electric and perpendicular magnetic fields, *Journal of Physics: Condensed Matter* **19**, 406231 (2007).
- [23] A. Shytov, M. Rudner, N. Gu, M. Katsnelson, and L. Levitov, Atomic collapse, lorentz boosts, klein scattering, and other quantum-relativistic phenomena in graphene, *Solid State Communications* **149**, 1087 (2009), recent Progress in Graphene Studies.
- [24] I. O. Niyi, V. Könye, S. G. Sharapov, and V. P. Gusynin, Landau level collapse in graphene in the presence of in-plane radial electric and perpendicular magnetic fields, *Phys. Rev. B* **106**, 085401 (2022).
- [25] N. Gu, M. Rudner, A. Young, P. Kim, and L. Levitov, Collapse of landau levels in gated graphene structures, *Phys. Rev. Lett.* **106**, 066601 (2011).
- [26] I. M. Lifshitz and M. I. Kaganov, Some problems of the electron theory of metals i. classical and quantum mechanics of electrons in metals, *Soviet Physics Uspekhi* **2**, 831 (1960).
- [27] A. Alexandradinata and L. Glazman, Semiclassical theory of landau levels and magnetic breakdown in topological metals, *Physical Review B* **97**, 144422 (2018).
- [28] E. C. Titchmarsh, *The Theory of the Riemann Zeta-Function* (Oxford Science Publications, 1987).